Climate Dynamics (2005) 24: 497–510
DOI 10.1007/s00382-004-0497-7

Nicola Stuber · Michael Ponater · Robert Sausen

Why radiative forcing might fail as a predictor of climate change

Received: 10 August 2004 / Accepted: 5 November 2004 / Published online: 15 February 2005

Abstract Radiative forcing has been widely used as a metric of climate change, i.e. as a measure by which various contributors to a net surface temperature change can be quantitatively compared. The extent to which this concept is valid for spatially inhomogeneous perturbations to the climate system is tested. A series of climate model simulations involving ozone changes of different spatial structure reveals that the climate sensitivity parameter λ is highly variable: for an ozone increase in the northern hemisphere lower stratosphere, it is more than twice as large as for a homogeneous CO_2 perturbation. A global ozone perturbation in the upper troposphere, however, causes a significantly smaller surface temperature response than CO_2. The variability of the climate sensitivity parameter is shown to be mostly due to the varying strength of the stratospheric water vapour feedback. The variability of the sea-ice albedo feedback modifies climate sensitivity of perturbations with the same vertical structure but a different horizontal structure. This feedback is also the origin of the comparatively larger climate sensitivity to perturbations restricted to the northern hemisphere extratropics. As cloud feedback does not operate independently from the other feedbacks, quantifying its effect is rather difficult. However, its effect on the variability of λ for horizontally and vertically inhomogeneous perturbations within one model framework seems to be comparatively small.

Keywords Radiative forcing · Climate feedbacks

This revised version was published online March 2005 with corrections to table 5.

N. Stuber · M. Ponater · R. Sausen
DLR-Institut für Physik der Atmosphäre,
Oberpfaffenhofen, Germany

N. Stuber (✉)
Department of Meteorology,
The University of Reading, Reading, UK
E-mail: N.Stuber@reading.ac.uk

1 Introduction

The ultimate goal of the United Nations Framework Convention on Climate Change (UNFCCC) is a "stabilization of greenhouse gas concentrations in the atmosphere at a level that would prevent dangerous anthropogenic interference with the climate system" (UNFCCC, Art. 2). The most straightforward way to achieve this goal is to reduce anthropogenic greenhouse gas emissions. Accordingly, the parties to the Kyoto Protocol agreed to reduce their "aggregate anthropogenic carbon dioxide equivalent emissions" (Art. 3,1) of six greenhouse gases or groups of gases, by at least 5% below the 1990 levels in the commitment period 2008–2012. As reductions in one of the gases are deducted from the total emission reduction commitment, a tool is needed to compare the different climatic impacts of different anthropogenic emissions. The key instrument of the Kyoto Protocol is the global warming potential GWP, which is the ratio of two time-integrated radiative forcings caused by decaying pulse emissions of radiatively active species (Ramaswamy et al. 2001). Radiative forcing (RF) gives a first-order estimate of the expected equilibrium global mean surface temperature change ΔT_{surf} caused by a radiatively active perturbation, e.g., an increase in atmospheric carbon dioxide concentration. Based on the experience from experiments with changes of the carbon dioxide concentration and the solar constant, the radiative forcing concept assumes a linear relationship between global mean radiative forcing and the global mean surface equilibrium temperature response

$$\Delta T_{\mathrm{surf}} = \lambda \cdot RF \tag{1}$$

If the model-dependent climate sensitivity parameter λ is known, a radiation imbalance RF can be translated into the resulting global mean temperature response without the need to actually conduct computationally expensive simulations with a comprehensive climate model. How-

ever, the concept only holds if the climate sensitivity parameter λ is sufficiently constant given different climate change mechanisms (greenhouse gases, aerosols, albedo, solar constant, etc.) as well as different spatial structures of the perturbations (tropospheric/stratospheric perturbations, perturbations in high/low latitudes, etc.).

Recently, it has been found that for some spatially inhomogeneous distributed forcings the climate sensitivity parameter is not a constant—even within one given model configuration. Different reasons for the nonlinearity between climate forcing and climate response have been discussed. Bintanja et al. (1997), using a simplified climate model, analysed the differences in the climate response to horizontally homogeneous and inhomogeneous perturbations. They showed that the comparatively higher λ for horizontally inhomogeneous perturbations with maximum forcing in high latitudes is due to the comparatively stronger sea-ice albedo feedback. Hansen et al. (1997) conducted experiments with a variety of differently structured perturbations, among them ozone added to individual model layers. They got a factor of eight spread between climate sensitivities to different perturbations. Part of this considerable variability of λ could be attributed to the variability of the cloud feedback.

Given the model dependence of the climate sensitivity parameter, Joshi et al. (2003) analysed the climate response to idealised perturbations using three quite different general circulation models. They found the variability of the climate sensitivity parameter to be quite large for the various perturbations and models. However, normalised by the climate sensitivity parameter for a reference case (homogeneous CO_2 increase), the climate sensitivity parameters stayed within 30% of each other for all models. Moreover, their results have indicated generic deviations of λ from the reference value. For example, extratropical perturbations yielded a significantly higher climate sensitivity parameter than tropical perturbations. Joshi et al. (2003) attributed this phenomenon partly to the distinctive latitudinal variation of outgoing longwave radiation. A similar conclusion was drawn by Mickley et al. (2004).

While Joshi et al. (2003) examined the climate response mainly to changes in upper tropospheric ozone, in the present study, we analyse a larger number of ozone perturbations that are inhomogeneous both vertically and horizontally. In a former study (Stuber et al. 2001b; hereafter SPS), we found that a large part of the variability of λ can be attributed to the variability of the stratospheric water vapour feedback. In view of the results of Bintanja et al. (1997) and Hansen et al. (1997), we have extended our analysis to include the sea-ice albedo and cloud feedback.

In the following sections, we will first give a brief overview of the model and summarise the ozone perturbations we used. A summary of the equilibrium response of several climate parameters is given in Sect. 3. In Sect. 4, we present results from two different approaches to quantify the influence of feedbacks. The paper ends with a discussion and conclusions.

2 Model description and experiments

We used the state-of-the-art general circulation model ECHAM4 in a version with T30 spectral horizontal resolution and with 19 vertical layers between the surface and the top layer centred at 10 hPa. (See Roeckner et al. 1996 for a detailed model description.) For the climate simulations, the model was coupled to a mixed layer ocean model of 50 m and to a thermodynamic sea-ice model. Trace gas concentrations and/or distributions are prescribed. However, water vapour is fully interactive and is advected by a semi-Lagrangian scheme. As the model configuration does not include a chemistry model, there is no stratospheric water vapour source from the oxidation of methane.

The ''stratosphere adjusted radiative forcing at the tropopause'', *RF*, was calculated online in the 3D GCM, according to Stuber et al. (2001a). For convenience, we will use the shortform ''radiative forcing''. Forster et al. (2001) conducted a dedicated check of the ECHAM4 radiation scheme. They found that the long wave forcing due to a realistic stratospheric ozone change, like the observed ozone depletion between 1979 and 1997, is underestimated by about 20%.

We imposed highly idealised, vertically inhomogeneous, positive perturbations on the ozone concentration in the GCM (Table 1). All perturbations were normalised to give a radiative forcing of roughly 1 W/m^2. For comparison, note that the tropospheric ozone

Table 1 Model layers, pressure (hPa) and strength (DU) of the ozone perturbations in the lower stratosphere (LS), upper (UT), middle (MT) and lower (LT) troposphere

Perturbation	Model layers	Height (hPa)	Horizontally homogeneous	Horizontally inhomogeneous	
				30°N–60°N	60°N–90°N
LS	2–4	20–86	315 DU	2600 DU	4340 DU
UT	8–10	220–460[a]	30 DU	150 DU	260 DU
MT	10–12	350–650	34 DU	190 DU	315 DU
LT	16–19	880–1013	114 DU	460 DU	910 DU

[a]Note that this only applies to the horizontally inhomogeneous (extratropical) UT perturbation, as the horizontally homogeneous UT perturbation follows the latitudinal shape of a time mean tropopause

increase since pre-industrial times leads to a *RF* of 0.3–0.6 W/m^2 (e.g., Hauglustaine et al. 1994; Roelofs et al. 1998; Roeckner et al. 1999), with up to 0.8 W/m^2 to be expected at the end of the twenty-first century (Gauss et al. 2003). A doubling of the carbon dioxide concentration results in a forcing of about 4 W/m^2(Hansen et al. 1997; Forster et al. 2000). Choosing a forcing as large as 1 W/m^2 greatly reduces the statistical uncertainty of ΔT_{surf}(Eq. 1), which has been a problem in studies with ozone perturbations of more realistic strength (Ponater et al. 1999; Stuber et al. 2001a). It has also been shown, in the latter paper, that at least for the case of a CO_2 perturbation the climate sensitivity is not severely dependent on the strength of the perturbation.

All ozone perturbations (Table 1) are constructed to be vertically inhomogeneous, i.e., restricted to model layers in the lower stratosphere (abbreviated as LS), upper troposphere (UT), middle troposphere (MT) and lower troposphere (LT), respectively. We conducted experiments with horizontally homogeneous ($_{hom}$) as well as horizontally inhomogeneous ($_{inhom}$) ozone perturbations. The latter ones are restricted to the northern hemisphere extratropics and have a relative maximum northwards of 60°N. For reference and comparison, we used a homogeneous carbon dioxide perturbation as well (denoted as "CO2"). Note that the horizontally homogeneous ozone perturbation in the upper troposphere (UT_{hom}) follows the shape of a mean tropopause and is not restricted to globally uniform, fixed model layers, in contrast to the other ozone perturbations. The spatial structure of most of the perturbations has no analogy in nature. One exception is an ozone increase in the lower stratosphere of the northern hemisphere extratropics. The height of this perturbation matches the height of the observed ozone decrease (Bojkov and Fioletov 1997; Steinbrecht et al. 1998), but the amount of ozone change is much larger. The northern hemisphere upper tropospheric ozone increase pattern resembles the one caused by aircraft NO_x emissions (Grewe et al. 2001).

All climate simulations have been extended over 30 years after spin-up. Additionally, we performed a 60-years control run (CTRL), which simulates the climate of the 1990s. The climate response was calculated relative to CTRL. The CTRL simulation also provides a measure of internal variability. We used the interannual standard deviation with 22 degrees-of-freedom to calculate confidence intervals for the mean responses. The number of degrees-of-freedom was estimated from an autocorrelation analysis according to Zwiers and von Storch (1995).

3 Results

Table 2 summarises the climate sensitivity parameters λ (mean) and their 95% confidence intervals for the various perturbations. As *RF* has no noticeable interannual variability, it can be regarded as quasi-constant and the confidence intervals for λ were derived from the standard deviation of T_{surf}. Note that, as *RF* was chosen to be unity, λ and global mean, annual mean ΔT_{surf} amount to the same value.

Table 2 Climate sensitivity parameter λ(in K /(Wm^{-2})) for the various perturbations. In addition to the mean values the 95% confidence intervals are given

Exp	λ (mean)	λ (95 %)	Exp	λ (mean)	λ (95 %)
LS_{hom}	1.46	[1.44; 1.48]	LS_{inhom}	1.83	[1.81; 1.85]
UT_{hom}	0.58	[0.56; 0.60]	UT_{inhom}	0.87	[0.85; 0.89]
MT_{hom}	0.92	[0.90; 0.94]	MT_{inhom}	1.10	[1.08; 1.12]
LT_{hom}	0.83	[0.81; 0.85]	LT_{inhom}	1.34	[1.32; 1.36]
CO2	0.81	[0.78; 0.83]			
-0.5 LS_{hom}	1.04	[0.98; 1.10]			

As expected, the global mean climate response to radiative forcings of equal amount but different spatial structures is far from being uniform. The calculated climate sensitivity parameters differ significantly from each other — with the exception of λ (LT_{hom}) and λ(CO2). Within our set of experiments, the sensitivity of the model to different perturbations varies by a factor of three. This is the same order of magnitude as the variability Cess et al. (1990) and Joshi et al. (2003) found for the response of different models to one given perturbation.

With the exception of the UT_{hom} perturbation, the model is more sensitive to ozone perturbations than to an equivalent carbon dioxide perturbation. Comparing perturbations at a specific height, the model is more sensitive to an ozone increase in the northern extratropics than to the corresponding horizontally homogeneous perturbations. The difference is most pronounced for an ozone increase in the lower troposphere (LT), for which climate response is 60% higher if the perturbation is not horizontally homogeneous but restricted to the northern hemisphere extratropics. This qualitatively confirms results reported by Bintanja et al. (1997) from a much simpler, mechanistic model.

The model response is most sensitive to ozone increases in the lower stratosphere, for which λ is twice that of CO2. Due to the large cancellation of shortwave and longwave effects the LS ozone increase has to be quite large to result in a 1 W/m^2 forcing (see Table 1). Hence, we tested the robustness of the LS result by an additional experiment with an overall 50% ozone reduction in the lower stratosphere ($-0.5LS_{hom}$, Table 2). This experiment deviates from our usual normalisation as the *RF* yields -0.34 W/m^2, but it qualitatively confirms the evidence of a higher climate sensitivity to ozone changes in the lower stratosphere compared to homogeneous CO_2 changes. An enhanced model sensitivity to ozone perturbations has also been reported by Forster and Shine (1999) for the observed stratospheric ozone decrease between 1979 and 1997, and by Stuber et al. (2001a) for—comparably small—aircraft-induced ozone changes in the UT/LS region. According to Joshi

et al. (2003), this latter finding might be due to the stratospheric component of the ozone increase, as well as due to the meridional structure of the perturbation with a strong maximum in the northern hemisphere extratropics. However, for a global upper tropospheric ozone increase just below the tropopause the climate response is 30% smaller than for an equivalent CO_2-perturbation (UT_{hom} in Table 2).

Figure 1 provides an impression of the spatial structure of the annual mean, zonal mean equilibrium temperature response for the various perturbations. We omitted the results for the MT perturbations, as they provide little additional information. For the horizontally inhomogeneous perturbations the temperature response is quite asymmetric with respect to the hemispheres. At all levels, temperature response is more pronounced in the northern hemisphere extratropics than southwards of 30°N.

For the ozone perturbations in the lower stratosphere a strong stratospheric warming is found, which also penetrates down into the upper troposphere. Temperature increase in the region of the ozone increase reaches up to 34 K for the LS_{inhom} perturbation. This strong temperature response is due to the comparably large

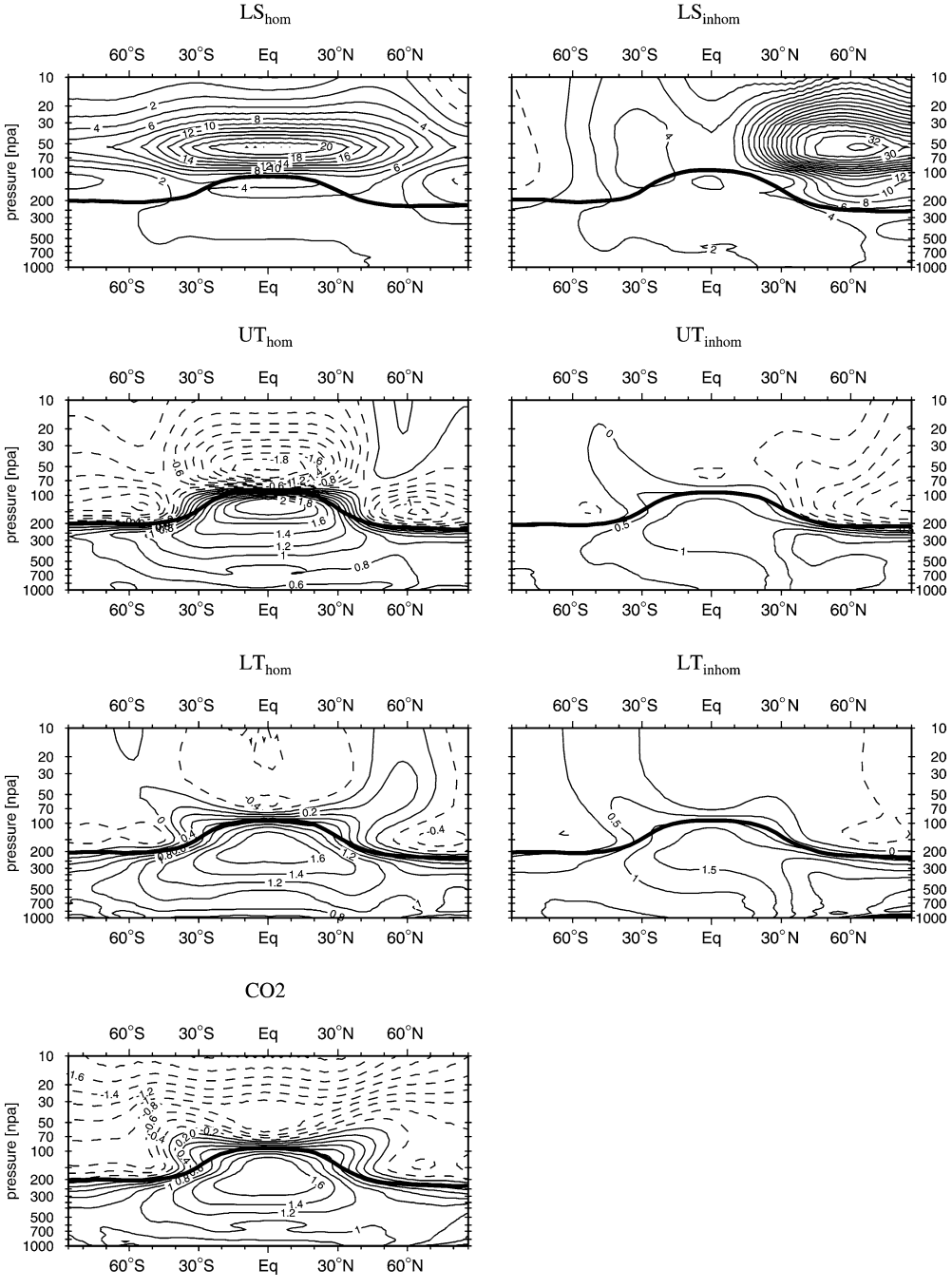

Fig. 1 Annual, zonal mean temperature response in K. Contour interval: 2 K (LS_{inhom}, LS_{hom}), 0.5 K (UT_{inhom}, LT_{inhom}) or 0.2 K, respectively

stratospheric ozone perturbation. The comparatively large ozone perturbation leads to high shortwave radiative absorption and a strong local radiative heating of the thin air at lower stratosphere altitudes.

For tropospheric ozone increases the temperature response features a dipole structure. Screening of shortwave and (terrestrial) longwave radiation leads to a stratospheric cooling (Ramaswamy and Bowen 1994), the greenhouse effect of tropospheric ozone perturbations results in a tropospheric warming.

Surface warming is largest in high latitudes for all experiments including CO2. This is known to be due to the temperature-sea ice feedback. However, as a result of the meridional structure of the perturbations, for the horizontally inhomogeneous ozone perturbations surface warming is even more pronounced in high northern latitudes.

Water vapour is known to work as an amplifier of externally forced warming as it is strongly coupled to surface temperature and evaporation. We take a closer look at the water vapour response in our experiments in Fig. 2, which shows the equilibrium change in water vapour mixing ratio relative to the control run distribution.

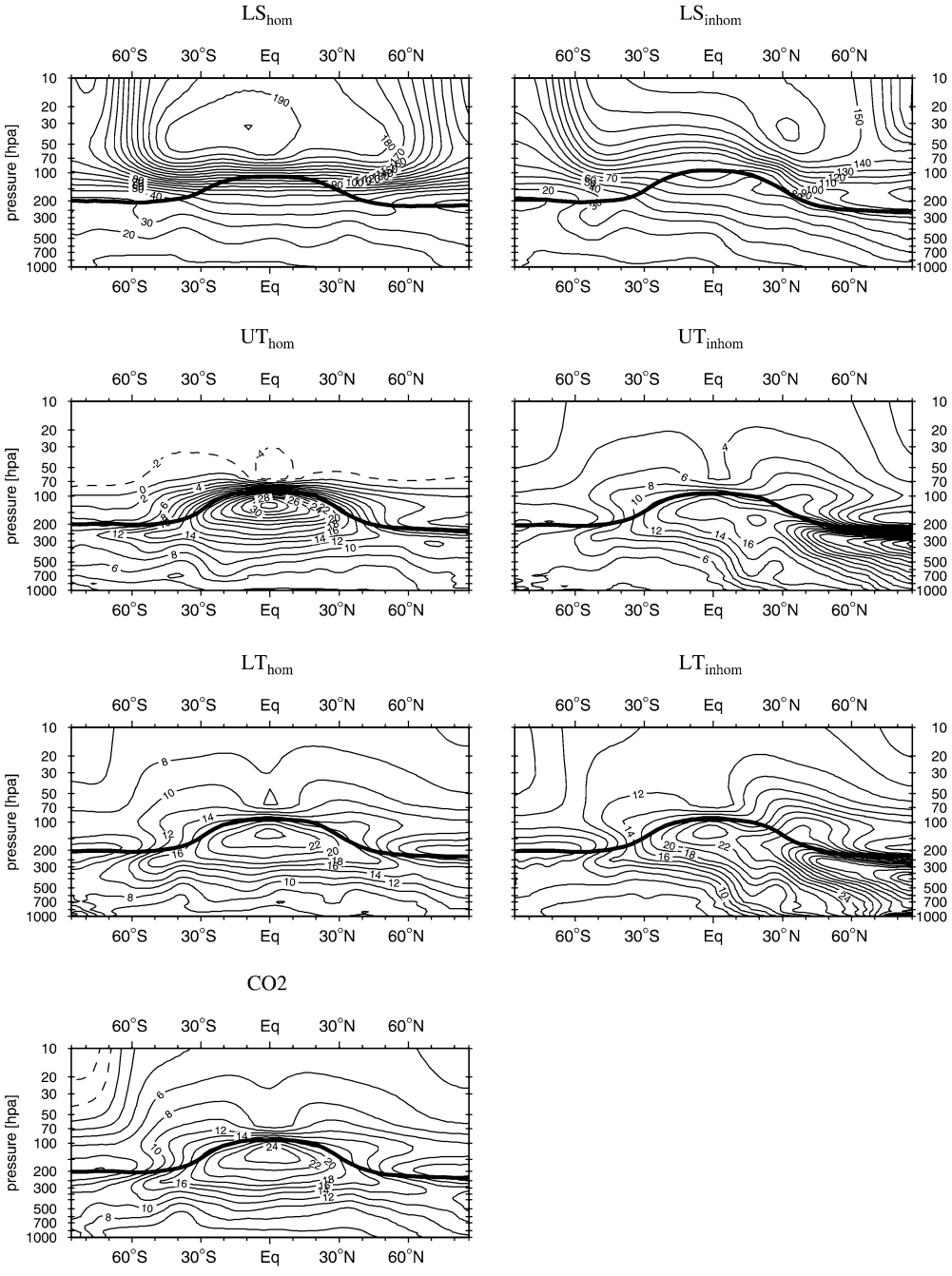

Fig. 2 Annual, zonal mean water vapour mixing ratio response relative to the control run distribution in %. Contour interval: 10% (LS$_{inhom}$, LS$_{hom}$), and 2% (other cases), respectively

With the exception of the response to the UT_{hom} perturbation, water vapour content increases throughout the whole atmosphere for all perturbations. Due to the large background concentration, the relative change in water vapour mixing ratio is comparably small in the troposphere and in the range of 30%. Over large parts of the troposphere, below approximately 400 hPa, water vapour response is straightforward and specific humidity increases almost linearly with surface temperature increase (cf., Fig. 1). Consistent with current global warming concepts, the relative humidity (not shown) in the troposphere is constant within a 2% range in all experiments and, thus, hardly sensitive to surface temperature changes.

However, stratospheric water vapour response to the different perturbations exhibits a unique signature for each perturbation. For the pair of ozone perturbations in the lower stratosphere, water vapour doubles over most of the stratosphere and even almost triples locally. For the LS_{hom} perturbation relative water vapour response is largest in the tropics. Equilibrium water vapour response to the LS_{inhom} perturbation is—like temperature response—more asymmetric in nature, with the largest relative increase of stratospheric water vapour slightly north of 30°N.

For the ozone perturbations just below the tropopause (UT), the sign of the stratospheric water vapour response crucially depends on the horizontal structure of the perturbation. An ozone increase in the northern hemisphere extratropics results in a moderate increase of stratospheric water vapour, whereas the globally extending UT_{hom} perturbation results in a water vapour decrease of about 2–4% over large parts of the stratosphere.

The unique signature of stratospheric water vapour response gives reason to suspect an equally unique signature of at least some of the different processes governing stratospheric water vapour content. Though these mechanisms are still controversial (see, e.g., the discussion in Sherwood and Dessler 2000), it is agreed on that stratospheric water vapour distribution is controlled by cold temperatures near the tropical tropopause (Brewer 1949; Holton et al. 1995). As air reaches saturation at the tropical tropopause, it is freeze-dried as it enters the stratosphere. Besides other mechanisms, e.g., an enhanced transport, changes in thermodynamics at the tropopause are of utmost importance for stratospheric water vapour distribution. Due to the strong non-linearity of the Clausius–Clapeyron equation, a change in the temperature minimum of the vertical profile leads to a significant change in the saturation mixing ratio (SMR) with respect to ice and, hence, in the amount of freeze drying.

To get an impression of this effect, we calculated for the various perturbations the changes in area-averaged tropical vertical temperature minimum CPT (cold point tropopause temperature) and SMR. Results are presented in Table 3 and Fig. 3. We are well aware that tropical mean tropopause temperatures are too high to explain the observed water vapour mixing ratio values (e.g., Holton 1984). Actually the mean CPT of the control run simulation (198.9 K) suggests a mean saturation volume mixing ratio of 13.8 ppmv, which is almost a factor three higher than the water vapour mixing ratio actually observed in the stratosphere (e.g., Michelsen et al. 2000) as well as simulated by the GCM (about 3.5 ppmv; not shown). This discrepancy may be

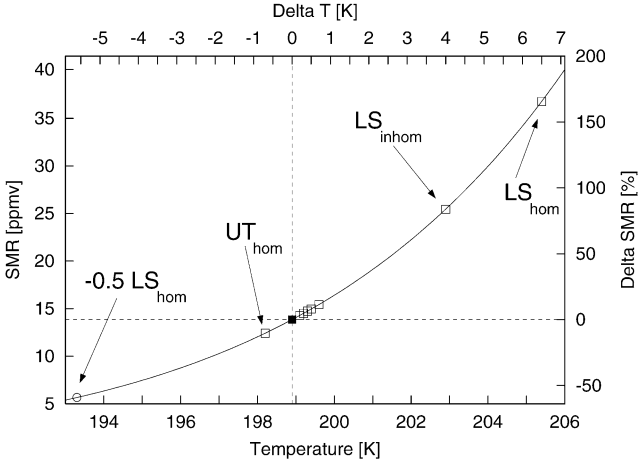

Fig. 3 Saturation mixing ratio (SMR) as a function of temperature (calculated according to Salby 1996). The values for the various experiments are marked with *open squares* and the CTRL value with a *filled square*, respectively. The value for the −0.5 LS_{hom} experiment, which conceptually deviates from the other experiments, is marked with an *open circle*

Table 3 Changes in tropical cold point temperature CPT, saturation mixing ratio (ΔSMR) over ice and stratospheric water vapour mass above 70 hPa (ΔH_2O), the latter two in percent of the control run values

Exp	ΔCPT (K)	ΔSMR (%)	ΔH_2O (%)	Exp	ΔCPT (K)	ΔSMR (%)	ΔH_2O (%)
LS_{hom}	6.5	165.8	177	LS_{inhom}	4.0	83.9	140
UT_{hom}	−0.7	−10.3	−2	UT_{inhom}	0.3	4.8	5
MT_{hom}	0.2	3.2	6	MT_{inhom}	0.5	8.1	7
LT_{hom}	0.5	8.1	9	LT_{inhom}	0.7	11.5	12
CO2	0.4	6.4	7				
−0.5 LS_{hom}	−5.6	−59.1	−35				

Saturation mixing ratios have been calculated from CPT according to Salby (1996). (For reference: CPT (CTRL) = 198.9 K; SMR(CTRL) = 13.8 ppmv, H_2O (CTRL) = 8×10^{11} kg)

caused by the difficulty to derive an effective CPT, averaged over space and time, from the archived temperature fields of the simulation. Nevertheless, the change in CPT may serve as a first, indicative measure of the effects of spatially inhomogeneous perturbations on near tropopause thermodynamics and, hence, on stratospheric water vapour content. In order to account for the response in tropopause height, we calculated the (relative) change in water vapour mass above a reference level of 70 hPa (Table 3). As zonal mean temperature response already suggests, ozone perturbations in the lower stratosphere result in a strong warming of the tropical tropopause region. For the LS_{hom} perturbation, CPT increases by 6.5 K and the SMR more than doubles as a consequence. Changes in tropical CPT are also sufficient to explain the differences in stratospheric water vapour response to horizontally inhomogeneous and homogeneous ozone perturbations in the upper troposphere (UT).

In general, stratospheric water vapour response seems to be mainly a function of the altitude of the ozone perturbation rather than the tropospheric or surface temperature response. Horizontal structure is a minor factor, though we have noted that it is of a vital importance for the response to an upper tropospheric ozone increase.

As both the global mean and the zonal mean surface temperature response are quite variable within the set of experiments (see Table 2 and Fig. 1), it stands to reason that sea-ice response depends on the spatial structure of the perturbations as well. Obviously, a change in either sea-ice cover or sea-ice thickness leads to a change in sea-ice volume, which in turn may serve as a measure of the energy actually spent on melting ice. In the following, we will confine the discussion on the response of sea-ice volume (Table 4).

For the horizontally inhomogeneous ozone perturbations, sea-ice response is—like temperature response—quite asymmetric. Up to 90% of global sea-ice reduction is due to the melting of Arctic sea-ice only. In general, reduction of Arctic sea-ice volume is larger for the ozone perturbations in the northern extratropics than for the respective horizontally homogeneous perturbations. This applies to global sea-ice response as well as the large northern hemispheric sea-ice reduction dominates the global response. The comparatively larger sea-ice reduction resulting from the horizontally inhomogeneous ozone increases is a result of the perturbations covering polar latitudes (Forster et al. 2000) as well as being restricted to the northern hemisphere extratropics (Bintanja et al. 1997). For the tropospheric ozone perturbations, global sea-ice response decreases with height of the ozone perturbation. The response for the LS perturbation seems to be comparatively large, but this should be related to the stronger overall surface heating. Hence, unlike the stratospheric water vapour response, the characteristic signature of the sea-ice response seems to be largely determined by the horizontal, i.e., meridional structure of the perturbation.

4 The effect of feedbacks on climate response and climate sensitivity

As we have demonstrated, the response of some key climate parameters, temperature, stratospheric water vapour, and sea-ice, is highly variable within the set of experiments. It stands to reason that the effect of the respective feedbacks on climate response is of equal distinctiveness. As a result, the variability of λ is likely to be strongly related to the variability of these feedbacks. Before quantifying the effect of different feedbacks on the net climate response, we briefly recall the theory of feedbacks, essentially following Hansen et al. (1984) and Schlesinger (1988).

4.1 Theory of feedbacks

The constraint of a balanced radiation budget at the top of the atmosphere requires that changes in radiatively active parameters lead to changes in climate, which is often represented by the (global mean) surface temperature change ΔT_{surf}. The resulting temperature change is a function of external as well as internal climate variables. Internal variables (e.g., water vapour content or cloud cover) are interactive parts of the changing climate-system: They provide feedbacks and modify the net climate response to an external forcing.

For simplicity, we assume that all internal variables are a function of surface temperature only. For the hypothetical case of a system without any feedbacks, the change in energy balance of the system is only a function of the external variables and of temperature, while other

Table 4 Equilibrium response of annual-mean northern and southern hemispheric and global sea-ice volume relative to the values of the control run, in percent. The ratio R is the fraction of global sea-ice volume reduction that is due to the melting of northern hemispheric (Arctic) sea-ice. For reference: the annual-mean global sea-ice volume in the control run is 32,000 km^3, the northern and southern hemisphere volumes are 15,000 and 17,000 km^3, respectively

Exp	Global (%)	SH (%)	NH (%)	R	Exp	Global (%)	SH (%)	NH (%)	R
LS_{hom}	−23.5	−13.5	−34.7	0.70	LS_{inhom}	−31.3	−13.2	−51.6	0.78
UT_{hom}	−11.3	−8.3	−14.6	0.61	UT_{inhom}	−18.0	−6.2	−31.1	0.82
MT_{hom}	−17.0	−11.9	−22.6	0.63	MT_{inhom}	−26.5	−5.4	−50.0	0.89
LT_{hom}	−19.1	−16.9	−21.5	0.53	LT_{inhom}	−37.2	−7.1	−70.7	0.90
CO2	−15.9	−12.9	−19.2	0.57					

internal variables do not interact. Under this assumption an external radiative forcing RF is directly transferred to the climate change $\Delta T_{\mathrm{surf}}(0)$ (see Fig. 4, top). The total climate forcing J is equal to the external forcing RF in Fig. 4, top. In a linear approximation we get

$$\Delta T_{\mathrm{surf}}(0) = \lambda_0 \cdot RF \tag{2}$$

with the constant of proportionality λ_0 being a measure of the gain of the system ($K/(Wm^{-2})$) in the absence of feedbacks.

However, in reality feedbacks are an integral part of the climate system and temperature change is not only the result of an external climate forcing but is modified by feedbacks. The mechanism of a feedback can best be illustrated by a simple block diagram (Fig. 4, bottom). Now the change and restoration of the energy balance is influenced by internal variables as well as by external variables and temperature. Part of the externally forced climate change is transferred through a feedback loop back to the input. Total climate forcing J is then given by the sum of the external forcing RF and some contribution ΔR from the feedback:

$$J = RF + \Delta R \tag{3}$$

In reality the climate system contains a multitude of feedbacks. In first-order approximation, we may assume that these M feedbacks are independent of each other. Such a chain of feedbacks can be linearised. As there are no interactions between the feedbacks, the combined effect of different radiative impacts to the system can be approximated by their sum. This leads to the climate response

$$\Delta T_{\mathrm{surf}} = \lambda_0 \cdot J = \lambda_0 \cdot \left(RF + \sum_i^M \Delta R_i \right) \tag{4}$$

For small perturbations, one may assume that the contributions ΔR_i depend linearly on the temperature change ΔT_{surf} such that $\Delta R_i = F_i \Delta T_{\mathrm{surf}}$. Inserting and solving for ΔT_{surf} gives

$$\Delta T_{\mathrm{surf}} = \frac{\lambda_0}{1 - \lambda_0 F} \cdot RF \equiv \lambda \cdot RF \tag{5}$$

where $F = \Sigma_i^M F_i$ represents the feedbacks. From this last equation, it becomes obvious how the climate sensitivity parameter λ depends on the feedbacks. The fact that feedbacks to the same external forcing are still simulated differently by different climate models makes λ a model dependent parameter (e.g., Cess et al. 1990).

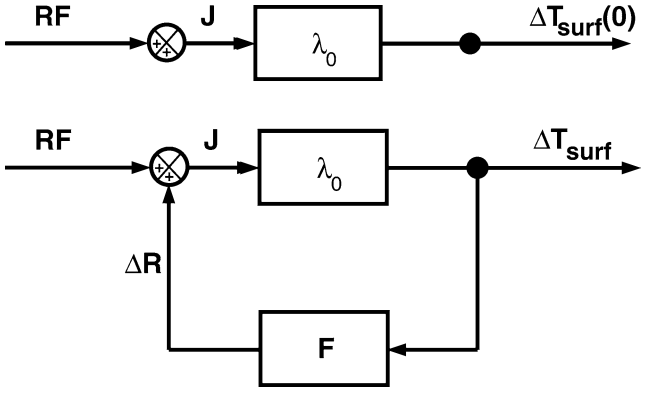

Fig. 4 Block diagram of the climate system without feedbacks (*top*) and with one feedback loop (*bottom*). *RF*: external climate forcing; ΔT_{surf}: temperature-response; $\Delta T_{\mathrm{surf}}(0)$: no-feedback temperature-response; λ_0: gain of the system in the absence of feedbacks; *F*: feedback; ΔR: contribution of the feedback to total climate forcing *J* (redrawn from Schlesinger 1988)

4.2 Quantifying the effect of feedbacks: diagnostic approach

According to our experimental design, the global external forcing RF is constant within the set of experiments. However, contributions ΔR_i from the feedbacks (see Eq. 4) are likely to be different, as the description of the equilibrium response of climate parameters (Sect. 3) has suggested. There are basically two different methods to quantify the contributions of single feedbacks to total climate forcing. In rather simple models, like the Wonderland model applied by Hansen et al. (1997), feedbacks may often be switched off individually to quantify their influence. In a comprehensive model such as ECHAM4, eliminating feedbacks is subject to some restrictions. Some feedbacks such as, e.g., cloud feedback with its various relations to convective transport, precipitation, etc., are too complex to be switched on and off. Beyond such conceptual problems, additional equilibrium climate simulations to estimate various feedbacks are quite costly. We, therefore, used results from climate runs with explicitly eliminated feedbacks only for a cross check of certain aspects of our findings (see Subsect. 4.3).

An alternative method to quantify the influence of certain feedbacks is to diagnose their contributions ΔR_i to total climate forcing J (Eq. 4). In accordance with the terminology of SPS, the ΔR_i will be referred to as "secondary forcings".

We are well aware that this diagnostic approach partly obscures the discrimination between (external) forcings and (internal) feedbacks. However, the approach is not so unusual as it may appear at first glance. A partial withdrawal from the strict distinction between external perturbations and the rather slow reaction of the climate system is already done when calculating the stratosphere adjusted radiative forcing. For good reasons stratospheric temperature response, which is, strictly speaking, a feedback, is regarded as an integral part of the forcing. Likewise, the feedback of externally forced aerosol changes in the troposphere to cloudiness is generally considered a forcing ("indirect aerosol forcing"; Twomey 1977; Rotstayn 1999) as well. It appears that there are "classical" feedbacks with a straightforward relation to surface temperature changes, like the tropospheric water vapour feedback (Schneider et al. 1999). However, as sea-ice and stratospheric water

vapour response exhibit a unique signature for primary forcings of different structure, they may be regarded as the cause of additional, "secondary" forcings.

The secondary forcings may be calculated from the equilibrium responses of sea-ice and stratospheric water vapour in exactly the same way as the *RF* resulting from the ozone or carbon dioxide perturbations. That is, we simply use the changes in stratospheric water vapour and sea-ice albedo as external perturbations and then calculate the resulting radiative forcings (see Stuber et al. 2001a, for further details). Table 5 summarises the respective results.

In accordance with the global sea-ice response (Table 4), secondary forcings from changes in sea-ice are larger for the perturbations restricted to the northern hemisphere extratropics than for the horizontally homogeneous ozone perturbations, confirming results by Bintanja et al. (1997). The quite dramatic decrease of Arctic sea-ice due to an ozone increase in the lower troposphere of the northern hemisphere extratropics (LT_{inhom}, see Table 4) is reflected in a maximum $RF(\Delta\alpha)$ of 17% of the primary greenhouse gas forcing, 11% are obtained for LS_{inhom}. For all other perturbations, the secondary forcings from the equilibrium change of sea-ice are more than one order of magnitude smaller than the radiative forcing due to the external greenhouse gas perturbation and up to one order of magnitude smaller than the secondary forcing from the equilibrium change of stratospheric water vapour.

As the equilibrium response of stratospheric water vapour (Fig. 2) already suggests, $RF(strat.\ \Delta q)$ is largest for the LS perturbations. For an ozone increase in the lower stratosphere the secondary forcing due to the doubling of stratospheric water vapour amounts to a similar magnitude as the radiative forcing due to the ozone increase (1 W/m^2). For all other perturbations, $RF(strat.\ \Delta q)$ is about one order of magnitude smaller.

Making the assumption that the feedbacks of stratospheric water vapour and sea-ice are in first-order approximation independent of each other—a prerequisite for the theory elucidated at the beginning of this Section—we can approximate the total climate forcing J with RF^*

$$RF^* = RF(O_3) + RF(\Delta_\alpha) + RF(strat.\Delta q) \quad (6)$$

Now, the sensitivity without the feedbacks of stratospheric water vapour and sea-ice may be approximated by the modified climate sensitivity parameter λ^*

$$\lambda^* = \frac{\Delta T_{surf}}{RF^*} \quad (7)$$

In calculating λ^*, we implicitly eliminate the influence of the two feedbacks on the simulated climate response. The results for λ^* and the 95% confidence intervals are summarised in Table 6. Note that unlike the idealised perturbations the mean changes in sea-ice and stratospheric water vapour are associated with a statistical uncertainty. In a preliminary study, we examined how the variability of the perturbations affects the variability of the resulting radiative forcings and, hence, the width of the confidence interval of λ^*. We found that the confidence interval of λ^* is dominated by the standard deviation of near surface temperature T_{surf}. Accordingly, the secondary forcings have been calculated from the long-time mean distributions of stratospheric water vapour and sea-ice and the secondary forcings are regarded as deterministic values without statistical uncertainty. The confidence intervals for λ^* have been calculated in the same way as those for λ from the standard deviation of T_{surf}.

Implicitly eliminating the two feedbacks reduces the model's sensitivity to all perturbations, as both feedbacks result in positive secondary radiative forcings. The effect is largest for the ozone perturbations in the lower

Table 5 Secondary radiative forcings due to the equilibrium changes in sea-ice (RF($\Delta\alpha$)) and stratospheric water vapour (RF($strat.\ \Delta q$))

Exp	$RF(\Delta\alpha)$ [W/m^2]	$RF(strat.\ \Delta q)$ [W/m^2]	Exp	$RF\ (\Delta\alpha)$ [W/m^2]	$RF\ (strat.\ \Delta q)$ [W/m^2]
LS_{hom}	0.051	1.113	LS_{inhom}	0.114	1.093
UT_{hom}	0.014	0.142	UT_{inhom}	0.032	0.156
MT_{hom}	0.024	0.167	MT_{inhom}	0.079	0.183
LT_{hom}	0.028	0.209	LT_{inhom}	0.172	0.277
CO2	0.021	0.193			

Table 6 Climate sensitivity parameters λ and modified climate sensitivity parameters λ^*, the latter resulting from an implicit elimination of feedbacks (sea-ice albedo, stratospheric water vapour), in $K/(Wm^{-2})$. The 95% confidence intervals have been derived from the standard deviation of T_{surf} (see text for details)

Exp	λ (mean)	λ^*(mean)	λ^*(95%)	Exp	λ (mean)	λ^*(mean)	λ^*(95 %)
LS_{hom}	1.46	0.68	[0.67; 0.69]	LS_{inhom}	1.82	0.84	[0.83; 0.85]
UT_{hom}	0.58	0.50	[0.49; 0.52]	UT_{inhom}	0.87	0.73	[0.71; 0.75]
MT_{hom}	0.92	0.77	[0.75; 0.79]	MT_{inhom}	1.10	0.88	[0.86; 0.89]
LT_{hom}	0.83	0.67	[0.66; 0.69]	LT_{inhom}	1.34	0.92	[0.91; 0.94]
CO_2	0.81	0.66	[0.65; 0.68]				

stratosphere for which climate sensitivity is halved. For the homogeneous CO_2 perturbation climate sensitivity decreases by about 18%. As we have suspected that these two feedbacks are the main reason for the non-linear relationship between radiative forcing and climate response, the variability of the calculated values λ^* should be significantly less than the variability of λ (Table 2). This is clearly evident from Table 6: λ^* varies only by a factor of 1.8 within the set of experiments, compared to a factor of 3 for λ. For two perturbations (LS_{hom} and LT_{hom}), the modified climate sensitivity parameters are even statistically undistinguishable from the respective value for the homogeneous carbon dioxide perturbation.

As noted above, we found sea-ice response and, hence, sea-ice albedo feedback, to be mainly determined by the horizontal structure of the ozone perturbations. Table 7 gives the climate sensitivity parameter λ for the northern extratropical ozone perturbations relative to λ for the horizontally homogeneous perturbations. The ratio is given for both, the all-feedback response, and for the climate response with feedbacks being implicitly eliminated.

As the values $R(\lambda^*)(\alpha)$ in Table 7 suggest, the variability of the sea-ice albedo feedback may already explain the largest part of the differences in the model sensitivity to horizontally differently structured perturbations.

However, the variations within our set of experiments (i.e., with horizontally homogeneous and horizontally inhomogeneous forcings), with a factor of 3 between the smallest and largest value of λ (Table 2), are larger than the variations between horizontally differently structured perturbations, which only amount up to a factor of 1.6.

Table 8 summarises "normalised climate sensitivity parameters" r. These give the climate sensitivity parameters for the various O_3 perturbations normalised with the climate sensitivity parameter for the homogeneous CO_2perturbation (see also Joshi et al. 2003). The values r give an impression of the underestimation or overestimation one might get by assuming a constant climate sensitivity parameter—e.g., the standard value for CO_2. As the values $R(\lambda^*)(\alpha)$ show, the variability within the set of experiments may not be explained solely by the variability of the sea-ice albedo feedback. This especially applies to the stratospheric ozone increases, for which $\lambda(O_3)$ and $\lambda^*(\alpha)(O_3)$ are more than 100% higher than the respective values for CO_2. After implicitly eliminating sea-ice albedo as well as stratospheric water vapour feedback, climate sensitivities lie within a factor of 1.8 of each other. This may be insufficient to save the assumption of constant climate sensitivity, but means a step to improved understanding as the original λ values vary by more than a factor of 3.

Table 7 Ratio of the climate sensitivity parameters for northern extratropical and homogeneous perturbations. $R(\lambda)$: ratio of the λ values (Table 2), $R(\lambda^*)(\alpha)$: ratio of the modified climate sensitivity parameters when only sea-ice albedo feedback is implicitly eliminated, $R(\lambda^*)(\alpha,str.\ q)$: ratio of the modified climate sensitivity parameters λ^*(Table 6) when both sea-ice albedo and stratospheric water vapour feedbacks are implicitly eliminated

Exp	$R(\lambda)$	$R(\lambda^*)(\alpha)$	$R(\lambda^*)(\alpha,str.\ q)$
LS	1.26	1.19	1.24
UT	1.49	1.47	1.45
MT	1.20	1.14	1.14
LT	1.61	1.41	1.38

4.3 Explicitly eliminated feedbacks

To test the significance and methodical robustness of these results we accomplished some additional model runs, in which the feedbacks of sea-ice and stratospheric water vapour were explicitly eliminated. Note that only the feedbacks on radiation were switched off. To this end, we forced the radiation scheme of the model to use the unperturbed distributions of stratospheric water vapour and sea-ice albedo while all other feedbacks were treated as before. Due to constraints on computer time, we had to restrict these additional climate simulations to the ozone perturbation in the lower stratosphere (LS_{hom}) and the homogeneous CO_2 perturbation. In addition to the runs with all feedbacks, we accomplished for both perturbations three runs with sea-ice albedo feedback and/or stratospheric water vapour feedback being explicitly eliminated. From the resulting temperature response, we calculated a climate sensitivity parameter with explicitly eliminated feedbacks, denoted as $\hat{\lambda}$ (Table 9).

For the homogeneous carbon dioxide perturbation, climate sensitivity decreases by about 8% when both feedbacks are eliminated. Temperature response due to the stratospheric water vapour feedback amounts to about 17% and sea-ice albedo feedback to about 83% of the combined effect of both feedbacks.

Regarding the ozone perturbation in the lower stratosphere, climate sensitivity almost halves (−46%) when both feedbacks are eliminated. This is mostly

Table 8 Normalised climate sensitivity parameters r for the various O_3perturbations when all feedbacks are active ($r(\lambda)$), and with sea-ice albedo feedback ($r(\lambda^*)(\alpha)$) or both sea-ice albedo and stratospheric water vapour feedbacks ($r(\lambda^*)(\alpha,\ str.\ q)$) being implicitly eliminated

Exp	$r(\lambda)$ (O_3/CO_2)	$r(\lambda^*)(\alpha)$ (O_3/CO_2)	$r(\lambda^*)(\alpha,\ str.\ q)$ (O_3/CO_2)
LS_{inhom}	2.28	2.09	1.26
UT_{inhom}	1.08	1.07	1.10
MT_{inhom}	1.37	1.30	1.32
LT_{inhom}	1.66	1.45	1.39
LS_{hom}	1.81	1.76	1.02
UT_{hom}	0.72	0.73	0.76
MT_{hom}	1.14	1.14	1.16
LT_{hom}	1.03	1.03	1.01

Table 9 Climate sensitivity parameter $\hat{\lambda}$ (means and 95% confidence intervals) in K/(Wm^{-2}) with the feedbacks of sea-ice (F_α) and/or stratospheric water vapour ($F_{str.\,q}$) on radiation being explicitly eliminated

		LS_{hom}			
		$F_{str.q}$			
F_α		1		0	
	1	1.455	1.435; 1.476	0.853	0.833; 0.874
	0	1.391	1.371; 1.411	0.785	0.765; 0.805
		CO_2			
		$F_{str.q}$			
F_α		1		0	
	1	0.805	0.784; 0.825	0.794	0.773; 0.814
	0	0.757	0.737; 0.777	0.743	0.723; 0.763

1: feedback on, *0*: feedback off. For comparison: $\lambda^*(\mathrm{LS_{hom}}) = 0.68$ K/(Wm^{-2}), $\lambda^*(CO_2) = 0.66$ K/(Wm^{-2})

(90%) due to the inactivated stratospheric water vapour feedback.

Note that for both perturbations, the combined effect of both sea-ice albedo and stratospheric water vapour feedback on radiation is given by the sum of the responses due to the individual feedbacks. This confirms that these two feedback mechanisms act largely independently of each other, justifying the above made assumption. The finding is also in line with results by Hansen et al. (1984) from experiments with a radiative convective model. However, they considered feedbacks not only on radiation, but on all other physical processes as well.

Eliminating the feedbacks of sea-ice albedo and stratospheric water vapour reduces the discrepancy between the model's sensitivity to the two perturbations, supporting the results from the diagnostic method. However, comparing the values of λ^* and $\hat{\lambda}$ reveals quantitative differences that are due to the conceptionally different approach in calculating λ^* and $\hat{\lambda}$. The basis for the calculation of modified climate sensitivity parameters λ^* are the equilibrium responses of sea-ice and stratospheric water vapour. The equilibrium distribution of stratospheric water vapour, for example, is not only a result of changed radiative fluxes, but of changes in transport, cloud formation, thermodynamic processes like dehydration in the tropics and various others as well. Additionally, a change in stratospheric water vapour will feed back on itself, e.g., as it changes tropical cold point temperature and, hence, stratospheric water vapour uptake. However, for calculating $\hat{\lambda}$we eliminate the feedback of stratospheric water vapour on radiation only. Not surprising, the resulting water vapour response (Fig. 5) is quantitatively quite different from the all-feedback response (Fig. 2).

Secondly, there are some discrepancies regarding the relative importance of the two feedbacks for the climate response on the homogeneous CO_2 perturbation. From the secondary forcings (Table 5), we might infer that stratospheric water vapour feedback ($RF(strat.\,\Delta q) = 0.193$) is far more important for climate response than sea-ice albedo feedback ($RF(\Delta\alpha) = 0.021$). However, the responses from climate runs with sea-ice albedo or stratospheric water vapour feedback being explicitly eliminated show an opposite behaviour. Most likely, the change in the radiative component of the sea-ice albedo feedback causes the other parts of the surface energy balance to change as well. Anyway, we conclude that the modified climate sensitivity parameters are indicative of the relative role of the feedbacks for the net equilibrium response, but their absolute values must be interpreted with caution.

4.4 Cloud feedback

The cloud feedback in climate sensitivity experiments is determined by changes in several parameters like cloud coverage, vertical distribution, optical depth or emissivity. All these parameters are highly variable in space and time, hence, diagnosing their combined effect by calculating secondary radiative forcings from the time-averaged equilibrium response is not straightforward. Moreover, a prognostic cloud scheme like that used in ECHAM is interacting in such a complex way with the hydrological cycle, the convective dynamics, and the radiation field that it becomes inpracticable to explicitly eliminate its feedback. Following Cess et al. (1996), we try to understand the role of the cloud feedback in our experiments by investigating the change in cloud radiative forcing, ΔCRF. We calculated CRF from long-term

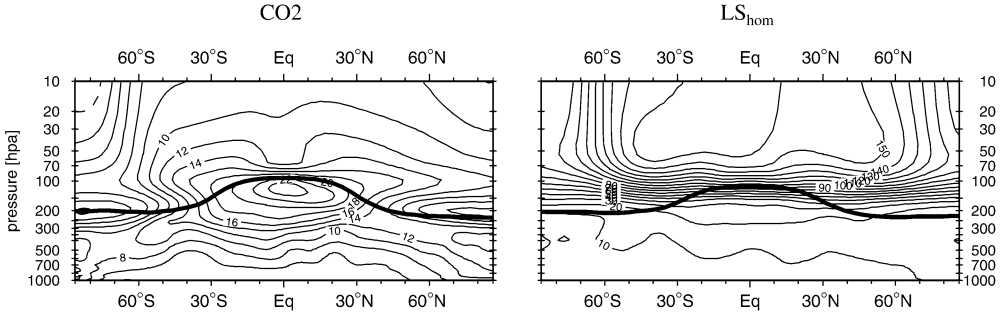

Fig. 5 Annual, zonal mean water vapour mixing ratio response relative to the control run distribution (in %) with the feedbacks of stratospheric water vapour and sea-ice albedo on radiation being explicitly eliminated. Contour interval: 2% (CO2) or 10% (LS$_{hom}$)

means of longwave and shortwave all-sky and clear-sky fluxes at the top of the atmosphere (Colman et al. 2001). The net cloud radiative forcing in the CTRL run is -20.3 W/m^2. The changes in the net *CRF* are summarised in Table 10.

In the CO2 experiment, the change in cloud forcing, ΔCRF, gives a negative feedback (-0.07 W/m^2), but it is too small to pass the test of statistical significance (at the 95% level). For the horizontally inhomogeneous ozone perturbations (except for UT_{inhom}), a significantly enhanced (i.e., less negative) cloud radiative forcing is caused, indicating that the cloud feedback supports the warming due to the increased ozone forcing in these experiments. This applies to the horizontally homogeneous perturbations in the middle and lower troposphere, too. In all these cases the cloud feedback acts in the same direction as the positive feedbacks of sea-ice albedo and (stratospheric) water vapour. However, a homogeneous ozone increase in the upper troposphere just below the tropopause (UT_{hom}) and in the lower stratosphere (LS_{hom}) gives a negative cloud feedback, i.e., a more effective cooling of the atmosphere-surface system. In these two cases, unlike the other experiments, a strong response of tropical cirrus occurs due to the substantial change in temperature and static stability around the tropical tropopause (Fig. 1). This results in either enhanced optical depth (LS_{hom}) or enhanced cloud cover (UT_{hom}), leading to higher albedo and an increased cooling of the system by a more negative shortwave *CRF* (not shown).

The cloud feedback, as far as it is represented by ΔCRF, cannot be interpreted as straightforward as the sea-ice albedo and stratospheric water vapour radiative feedback as it does not operate independent from the other feedbacks. This is most apparent for the LS_{hom} case, where the cloud radiative effect is not only modified by changes in the cloud parameters, but obviously by the humidity and temperature change at the cloud location as well. No doubt, the cloud feedback is important for the value of the basic sensitivity parameter λ in different climate models (e.g., Cess et al. 1996; Lee et al. 1997). However, from all the reasons mentioned above we do not recommend to quantify the influence of the cloud feedback to the climate sensitivity found in our various experiments in the same way as proposed in Sect. 4.2for the sea-ice albedo and stratospheric water vapour feedback. Reconsidering the values of λ^* in Table 6, it may be tempting to interpret the remaining excess of climate sensitivity found in the LT_{inhom}, MT_{inhom}, and LS_{inhom} experiments (compared to CO2) by the differences in cloud feedbacks. However, this approach fails to explain the difference between the comparatively large λ in LS_{hom} and the comparatively small λ in UT_{hom}, as ΔCRF is of the same sign and even of approximately the same magnitude in these cases (Table 7). We also note that in those LS_{hom} and CO2 experiments, in which the sea-ice albedo and stratospheric water vapour feedbacks have been switched off explicitly (q.v., Table 9), the cloud feedback, ΔCRF, amounts to $+0.21$ and $+0.23$ W/m^2, respectively. This large difference to the standard experiments emphasises how strong the interaction between the feedbacks due to water vapour and clouds appears to be.

We conclude that the equilibrium change of the cloud radiative forcing, ΔCRF, is in itself not an appropriate measure to explain differences in the climate sensitivity parameter between our various experiments in a sufficiently quantitative sense. ΔCRF is indicative, of course, of the direction, in which globally averaged cloud changes drive the temperature response of the climate system, but a more detailed look at the response of individual cloud parameters like optical depth, cloud water content or effective emissivity would be necessary to understand the underlying causes and effects. Differences in the 3D structure of the cloud response must probably be considered as well. Some of the relevant parameters are not available from the archive of the experiments discussed here, so a closer look to the quantitative impact of cloud processes must be postponed. Anyway, with respect to the sensitivity experiments we have considered here, the role of the cloud feedbacks does not appear to be the decisive one, as most of the variability of λ can be explained by other feedbacks.

Table 10 Changes in net cloud radiative forcing for the various experiments. The responses on the UT_{inhom} and CO2 perturbations are not statistically significant

Exp	ΔCRF(W/m^2)	Exp	ΔCRF(W/m^2)
LS_{hom}	-0.41	LS_{inhom}	0.42
UT_{hom}	-0.36	UT_{inhom}	–
MT_{hom}	0.21	MT_{inhom}	0.32
LT_{hom}	0.25	LT_{inhom}	0.42
CO2	–		

5 Summary and conclusions

As an extension of the work presented in Stuber et al. (2001b; "SPS"), we analysed the quantitative impact of different feedbacks on the varying climate responses in idealised ozone perturbation experiments. We diagnosed the contributions of sea-ice albedo and stratospheric water vapour feedback to climate sensitivity using the "secondary forcings", which can be calculated from the equilibrium responses of the respective parameters (cp., SPS). This diagnostic approach allows an implicit elimination of the feedbacks of sea-ice albedo and stratospheric water vapour from the net surface temperature response at very limited computational resources. It makes clear that the variation of the climate sensitivity parameter λ is substantially controlled by these two feedbacks. Experiments in which the ozone forcing implies a strong impact at the tropopause altitude produce a specific signature in the stratospheric water vapour

feedback and, subsequently, a specific behaviour of climate response and climate sensitivity. Additional climate simulations with the two feedbacks being explicitly eliminated qualitatively confirmed this finding.

Previous results of Bintanja et al. (1997) could be confirmed. The strength of the sea-ice albedo feedback is governed by the meridional structure of the forcing. Northern extratropical perturbations result in a comparably higher sea-ice albedo feedback as well as a higher climate sensitivity parameter than globally extending perturbations with the same global mean radiative forcing. This is also in line with more recent results of Joshi et al. (2003) and Mickley et al. (2004), though it must be noted that a considerable model dependency remains to be explored with respect to the relative climate sensitivity of ozone and CO_2 changes, respectively.

Hansen et al. (1997) suggested that the similarity of the responses to global CO_2 and solar constant forcings may be partly accidental. They proposed that the striking similarity of the global mean surface temperature response in these cases, which has been the basis for the radiative forcing concept, is due to the cancellation of two contrary effects: On the one side, climate being more sensitive to high-latitude than to low-latitude forcings (favouring the carbon dioxide forcing) and on the other side, climate being more sensitive to forcings initially being felt at the surface and lower troposphere (favouring the solar forcing). This is quite in line with the evidence we have reported here. Moreover, we found that heating rates and temperature changes near the tropical tropopause are slightly higher for an increase in the solar constant (not shown) than for the equivalent CO_2 perturbation. The resulting secondary forcing due to the increase in stratospheric water vapour is about 8% higher than for CO_2. In contrast, the increase in carbon dioxide concentration, with its forcing being more pronounced in high-latitudes, results in an about 5% higher secondary sea-ice forcing.

We made an attempt to quantify the impact of the cloud feedback by calculating the change in cloud radiative forcing *CRF* (Cess et al. 1996; Colman et al. 2001). Though it is indisputable that the cloud feedback modifies climate response, our results suggest that its effect on the variability of λ in the experiments discussed here is smaller than the sea-ice albedo and stratospheric water vapour feedbacks. However, the comparatively small climate sensitivity to an upper tropospheric ozone increase could be substantially affected by the negative cloud feedback: this reduced climate sensitivity can not be completely explained by the feedbacks of sea-ice albedo and stratospheric water vapour. Quantitative diagnosis of the role of the cloud feedback requires a more detailed study of individual cloud parameters (beyond coverage) like optical depth and emissivity. Some of these parameters were not available from the simulations performed for the present study, hence, this task will be approached in a subsequent paper.

Acknowledgements The authors wish to thank Keith Shine for thoroughly commenting on an early version of this paper. This study was funded through the project "Metric" within the FP5 program of the EU. We thank two anonymous reviewers for their helpful and stimulating comments.

References

Bintanja R, Fortuin JPF, Kelder H (1997) Simulation of the meridionally and seasonally varying climate response caused by changes in the ozone concentration. J Clim 10:1288–1311

Bojkov RD, Fioletov VE (1997) Changes of lower stratospheric ozone over Europe and Canada. J Geophys Res 102:1337–1347

Brewer AW (1949) Evidence for a world circulation provided by measurements of helium and water vapour distribution in the stratosphere. Q J R Meteorol Soc 75:351–363

Cess RD, Potter GL, Blanchet JP, Boer GJ, Del Genio AD, Déqué M, Dymnikov V, Galin V, Gates WL, Ghan SJ, Kiehl JT, Lacis AA, Le Treut H, Li Z-X, Liang X-Z, McAvaney BJ, Meleshko VP, Mitchell JFB, Morcrette J-J, Randall DA, Rikus L, Roeckner E, Royer JF, Schlese U, Sheinin DA, Slingo A, Solokov AP, Taylor KE, Washington WM, Wetherald RT, Yagai I, Zhangi M-H (1990) Intercomparison and interpretation of climate feedback processes in 19 atmospheric general circulation models. J Geophys Res 95:16601–16615

Cess RD, Zhang MH, Ingram WJ, Potter GL, Alekseev V, Barker HW, Cohen-Solal E, Colman RA, Dazlich DA, Del Genio AD, Dix MR, Dymnikov V, Esch M, Fowler LD, Fraser JR, Galin V, Gates WL, Hack JJ, Kiehl JT, Le Treut H, Lo KK-W, McAvaney BJ, Meleshko VP, Morcrette J-J, Randall DA, Roeckner E, Royer J-F, Schlesinger ME, Sporyshev PV, Timbal B, Volodin EM, Taylor KE, Wang W, Wetherald RT (1996) Cloud feedback in atmospheric general circulation models: an update. J Geophys Res 101:12791–12794

Colman R, Fraser J, Rotstayn L (2001) Climate feedbacks in a general circulation model incorporating prognostic clouds. Clim Dyn 18:103–122

Forster PM de F, Blackburn M, Glover R, Shine KP (2000) An examination of climate sensitivity for idealised climate change experiments in an intermediate general circulation model. Clim Dyn 16:833–849

Forster PM de F, Shine KP (1999) Stratospheric water vapour changes as a possible contributor to observed stratospheric cooling. Geophys Res Lett 26:3309–3312

Forster PM de F, Ponater M, Zhong WY (2001) Testing broadband radiation schemes for their ability to calculate the radiative forcing and temperature response to stratospheric water vapour and ozone changes. Meteorol Z 10:387-393

Gauss M, Myhre G, Pitari G, Prather MJ, Isaksen ISA, Berntsen TK, Brasseur GP, Dentener FJ, Derwent RG, Hauglustaine DA, Horowitz LW, Jacob DJ, Johnson M, Law KS, Mickley LJ, Müller J-F, Plantevin P-H, Pyle JA, Rogers HL, Stevenson DS, Sundet JK, van Weele M, Wild O (2003) Radiative forcing in the 21st century due to ozone changes in the troposphere and the lower stratosphere. J Geophys Res 108:10.1029/2002JD002624

Grewe V, Dameris M, Fichter C, Sausen R (2001) Impact of aircraft NOx emissions. Part I: interactively coupled climate-chemistry simulations and sensitivities to chemistry-climate feedback, lightning, and model resolution. Meteorol Z 11:177–186

Hansen J, Lacis A, Rind D, Russell G, Stone P, Fung I, Ruedy R, Lerner J (1984) Climate sensitivity: Analysis of feedback mechanisms. In: Hansen JE, Takahashi T (eds) Climate processes and climate sensitivity. American Geophysical Union, Washington DC, pp 130–163

Hansen J, Sato M, Ruedy R (1997) Radiative forcing and climate response. J Geophys Res 102:6831–6864

Hauglustaine DA, Granier C, Brasseur GP, Megie G (1994) The importance of atmospheric chemistry in the calculation of radiative forcing on the climate system. J Geophys Res 99:1173–1186

Holton JR (1984) Troposphere-stratosphere exchange of trace constituents: the water vapor puzzle. In: Holton JR, Matsuno T (eds) Dynamics of the middle atmosphere. Terra Sci, Tokyo, pp 369–385

Holton JR, Haynes PH, McIntyre ME, Douglass AR, Rood RB, Pfister L (1995) Stratosphere—troposphere exchange. Rev Geophys 33:403–439

Joshi M, Shine K, Ponater M, Stuber N, Sausen R, Li L (2003) A comparison of climate response to different radiative forcings in three general circulation models: towards an improved metric of climate change. Clim Dyn 20:843–854 DOI 10.1007/s00382-003-0305-9

Lee W-H, Iacobellis SF, Somerville RC (1997) Cloud radiation forcings and feedbacks: general circulation model tests and observational validation. J Clim 10:2479–2496

Michelsen HA, Irion FW, Manney GL, Toon GC, Gunson MR (2000) Features and trends in atmospheric trace molecule spectroscopy (ATMOS) version 3 stratospheric water vapor and methane measurements. J Geophys Res 105:22713–22724

Mickley LJ, Jacob DJ, Field BD, Rind D (2004) Climate response to the increase in tropospheric ozone since preindustrial times: a comparison between ozone and equivalent CO_2forcings. J Geophys Res 109:10.1029/2003JD003653

Ponater M, Sausen R, Feneberg B, Roeckner E (1999) Climate effect of ozone changes caused by present and future air traffic. Clim Dyn 15:631–642

Ramaswamy V, Bowen MM (1994) Effect of changes in radiatively active species upon the lower stratospheric temperatures. J Geophys Res 99:18909–18921

Ramaswamy V, Boucher O, Haigh J, Hauglustaine D, Haywood J, Myhre G, Nakajima T, Shi GY, Solomon S (2001) Radiative forcing of climate change. In: Houghton JT, Ding Y, Griggs DJ, Noguer M, van der Linden PJ, Dai X, Maskell K, Johnson CA (eds) Climate change 2001: the scientific basis. Contribution of working group I to the third assessment report of the intergovernmental panel of climate change. Cambridge University Press, Cambridge, pp 349–416

Roeckner E, Arpe K, Bengtsson L, Christoph M, Claussen M, Dümenil L, Esch M, Giorgetta M, Schlese U, Schulzweida U (1996) The atmospheric general circulation model ECHAM-4: model description and simulation of present-day climate. Max–Planck Institut für Meteorologie, Report no. 218. Hamburg, Germany

Roeckner E, Bengtsson L, Feichter J, Lelieveld J, Rodhe H (1999) Transient climate change simulations with a coupled atmosphere-ocean GCM including the tropospheric sulfur cycle. J Clim 12:3004–3032

Roelofs G-J, Lelieveld J, Feichter J (1998) Model simulations of the changing distribution of ozone and its radiative forcing of climate. Max–Planck Institut für Meteorologie report no. 283. Hamburg, Germany

Rotstayn L (1999) Indirect forcing by anthropogenic aerosols: a general circulation model calculation of the effective-radius and cloud lifetime effects. J Geophys Res 104:9369–9380

Salby ML (1996) Fundamentals of atmospheric physics. Academic, San Diego

Schlesinger ME (1988) Quantitative analysis of feedbacks in climate model simulations of CO_2-induced warming. In: Schlesinger ME (ed) Physically-based modelling and simulation of climate and climatic change: proceedings of the NATO Advanced Study Institute held in Erice, Italy, 11–23 May 1986, Kluwer, Dordrecht, pp 653–735

Schneider EK, Kirtman BP, Lindzen RS (1999) Tropospheric water vapor and climate sensitivity. J Atmos Sci 56:1649–1658

Sherwood SC, Dessler AE (2000) On the control of stratospheric humidity. Geophys Res Lett 27:2513–2516

Steinbrecht W, Claude H, Köhler U, Hoinka KP (1998) Correlations between tropopause height and total ozone: implications for long-term changes. J Geophys Res 103:19183–19192

Stuber N, Sausen R, Ponater M (2001a) Stratosphere adjusted radiative forcing calculations in a comprehensive climate model. Theor Appl Climatol 68:125–135

Stuber N, Ponater M, Sausen R (2001b) Is the climate sensitivity to ozone perturbations enhanced by stratospheric water vapor feedback? Geophys Res Lett 28:2887–2890

Twomey SA (1977) The influence of pollution on the shortwave albedo of clouds. J Atmos Sci 34:1149–1152

Zwiers FW, von Storch H (1995) Taking serial correlation into account in tests of the mean. J Clim 8:336–351